Epitaxial ordering of a perylenetetracarboxylic diimide-melamine supramolecular network driven by the Au(111)-$(22\times\sqrt{3})$ reconstruction

Fabien Silly,[1,2,a)] Adam Q. Shaw,[1] G. A. D. Briggs,[1] and Martin R. Castell[1,b)]
[1]*Department of Materials, University of Oxford, Parks Road, Oxford OX1 3PH, United Kingdom*
[2]*Zernike Institute for Advanced Materials, University of Groningen, 9747 AG Groningen, The Netherlands*

(Received 7 September 2007; accepted 12 December 2007; published online 14 January 2008)

Substrate mediated ordering and intermolecular interactions are used to create a long-range supramolecular network of perylenetetracarboxylic diimide and melamine on a reconstructed Au(111)-$(22\times\sqrt{3})$ surface. Scanning tunneling microscopy reveals that the network is composed of a succession of double width honeycomb cell rows separated by a more closely packed row of parallelograms. This periodicity of the supramolecular configuration matches that of the reconstructed gold substrate allowing an epitaxial relationship between network and substrate reconstruction. © *2008 American Institute of Physics*. [DOI: 10.1063/1.2830828]

The autonomous ordering and assembly of different molecules on atomically well-defined surfaces is an important technique for evolving applications in organic and molecular electronics. Long-range molecular ordering can be achieved by taking advantage of nanostructured substrates.[1–5] Another method exploits intermolecular interactions by mixing different molecular species to form extended networks.[5–9] The resulting supramolecular architecture can be tailored by modifying the functionality and the structure of the molecular building blocks. Further tuning can be achieved by changing the sample temperature[10] or relative molecular abundance during the preparation process. In our study, we have investigated the supramolecular network that forms through the combination of 1,3,5-triazine-2,4,6-triamine (melamine) and 3,4,9,10-perylenetetracarboxylic diimide (PTCDI). Previous work on this system has shown that an epitaxial honeycomb network evolves when the molecules are deposited on a silver terminated silicon surface[7] or Au(111) surface.[11,12] In our experiments, we show that the reconstruction of the Au(111)-$(22\times\sqrt{3})$ surface modifies and orders the honeycomb network. The result is a network of hexagons interspersed with rows of parallelograms that is epitaxial with the reconstruction of the gold substrate.

In our experiments, we used Au(111) films grown on mica as substrates. The samples were introduced into the ultrahigh vacuum (UHV) chamber of a scanning tunneling microscope (STM) (JEOL JSTM4500S) operating at a pressure of 10^{-8} Pa. The Au(111) surfaces were sputtered with argon ions and annealed in UHV at temperatures between 600 and 800 °C typically for 30 min. PTCDI molecules were sublimated at 335 °C and melamine at 100 °C. Etched tungsten tips were used to obtain constant current images at room temperature with a bias voltage applied to the sample.

Figure 1(a) shows a STM image of the Au(111) surface. This surface reconstructs into a complex structure composed of paired rows. If the atoms in the (111) plane of the face centred cubic (fcc) crystal retained their bulk positions, a flat hexagonal surface lattice would result. On Au(111) surfaces, a complicated interaction of short range and long range forces allows the surface atoms to shorten their nearest neighbor distances. This gives rise to changes in the atomic stacking sequence across the surface varying from unfaulted fcc stacking to faulted hcp stacking. The regular arrangements of the stacking faults produce a $(22\times\sqrt{3})$ surface unit cell with the fcc to hcp stacking boundaries running in the $\langle 11\bar{2}\rangle$ directions. Ideally, the Au(111) surface reconstructs into a "herringbone" pattern, but often it forms a complicated pattern of paired corrugation lines in different domains.[13] The bright lines visible in the STM image of Fig. 1(a) are the fcc to hcp boundaries where the surface gold atoms are located near bridge-site positions. The atoms on the bridge sites stand proud furthest from the surface and, therefore, appear bright in the STM images. The double ridge period is 6.3 nm, and the measured corrugation height in the STM image is 0.25 Å.

Figure 1(d) shows the supramolecular network that results after deposition of PTCDI and melamine onto the Au(111)-$(22\times\sqrt{3})$ surface followed by a postanneal at 80 °C for 15 h. The network is composed of a succession of double rows of hexagons and a single row of parallelograms. Each hexagon is formed from six melamine molecules and six PTCDI molecules, as shown in the diagram in Fig. 1(c). PTCDI and melamine are hydrogen bonded to each other through two O–H bonds and one N–H bond, as shown in Fig. 1(b). Previous experiments have shown that when PTCDI and melamine form a network on the Ag terminated Si(111) surface, an epitaxial honeycomb pattern is created that is entirely composed of hexagons.[7] For the Au(111)-$(22\times\sqrt{3})$ substrate in our experiments, a regular arrangement of non-hexagonal parallelogram units is incorporated into the network. The rows of parallelograms are indicated in Fig. 1(d) through gray and black arrows. The parallelogram rows are ~6.3 nm apart, which corresponds to the periodicity of the Au(111)-$(22\times\sqrt{3})$ reconstruction in the $[1\bar{1}0]$ direction. The periodicity of the hexagons along the rows was found to be 3.50 nm. Supramolecular network images that are similar to Fig. 1(d) but aligned in the two other crystallographically equivalent $\langle 11\bar{2}\rangle$ directions were obtained but are not shown here.

The STM image in Fig. 2(a) reveals the reconstructed Au(111)-$(22\times\sqrt{3})$ surface through a gap in the epitaxial PTCDI-melamine supramolecular network. The paired bright

a)Electronic mail: f.n.silly@rug.nl.
b)Electronic mail: martin.castell@materials.ox.ac.uk.

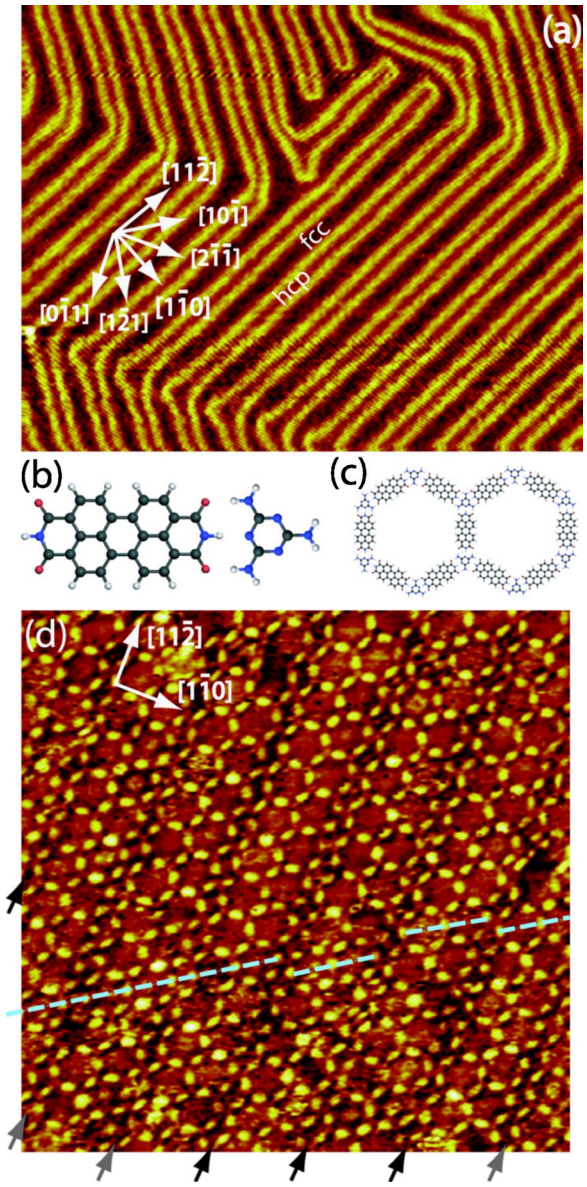

FIG. 1. (Color online) (a) STM image of the reconstructed Au(111)-$(22\times\sqrt{3})$ surface (80×67 nm^2, $V_s=-1.5$ V, $I_t=0.20$ nA). (b) PTCDI (left) and melamine (right) molecules. In the molecular representation, gray balls are carbon atoms, red balls are oxygen atoms, white balls are hydrogen atoms, and blue balls are nitrogen atoms. (c) Model of the combination of PTCDI and melamine which results in the honeycomb network. (d) STM image of the PTCDI-melamine supramolecular network grown on the reconstructed Au(111)-$(22\times\sqrt{3})$ surface. A succession of double width honeycomb cell rows can be seen, separated by a more closely packed row of parallelograms, as indicated by the arrows (50×50 nm^2, $V_s=-1.5$ V, $I_t=0.15$ nA).

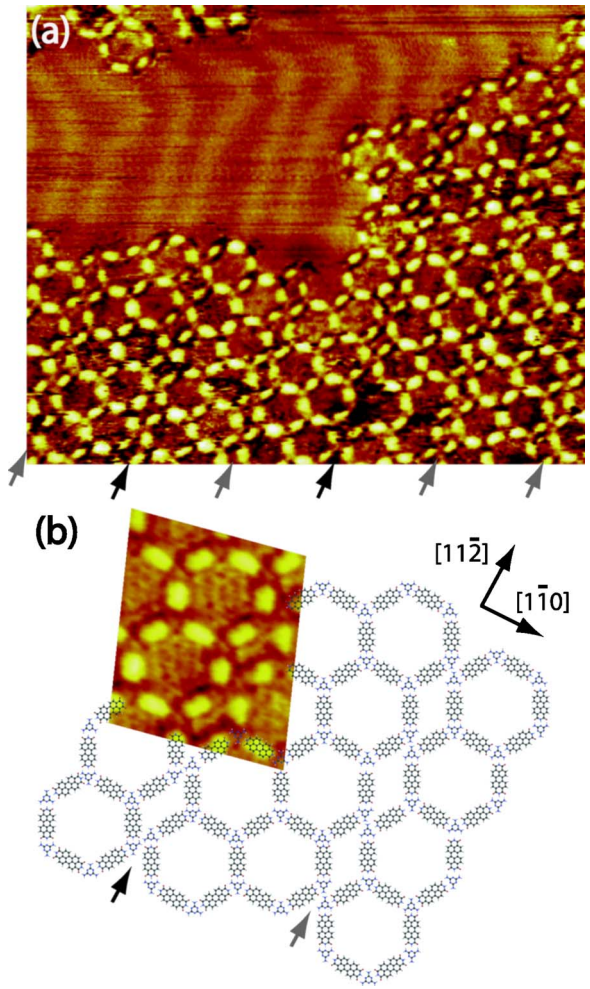

FIG. 2. (Color online) (a) STM image of a gap in the PTCDI-melamine supramolecular network revealing the reconstructed Au(111) substrate (50×35 nm^2, $V_s=-1.5$ V, $I_t=0.15$ nA). (b) Model of the supramolecular network with a superimposed high resolution STM image. The two types of parallelogram rows are indicated by black and gray arrows.

lines are clearly visible which correspond to the fcc-hcp boundaries on the gold surface. Such images, and similar ones from other parts of the sample, allow us to identify the geometrical relationship between the reconstructed substrate and the supramolecular network. We find that the parallelogram rows of the network [indicated by arrows in Figs. 1(d) and 2] line up with the fcc regions of the Au(111) reconstruction. The bright lines of Au(111), corresponding to bridge-site atoms, pass through the center of the hexagonal pores. The PTCDI molecules on these lines are aligned in the $[1\bar{1}0]$ direction, so that the PTCDI molecules are perpendicular to the bright lines of the Au(111) substrate. A model of the epitaxial PTCDI-melamine supramolecular network is presented in Fig. 2(b). Local packing of this type was previously reported by Perdigao *et al.*[11] who assumed that the molecular network lifts the Au(111) reconstruction. In the illustration, we have included both symmetries of the parallelogram boundaries, as indicated in Fig. 2(b) by black and gray arrows. A high resolution STM image of the network is superimposed on the model. In this image, PTCDI molecules are yellow and melamine brown.

Figure 2(b) shows that along the $[11\bar{2}]$ direction (the direction of the fcc-hcp boundaries), the periodicity of the hexagons is not disrupted. However, along the two other crystallographically equivalent directions, the $[1\bar{2}1]$ and $[2\bar{1}\bar{1}]$ directions, the hexagon periodicity is disrupted due to the parallelogram boundaries. This effect is illustrated in Fig. 1(d) where a dashed blue line has been drawn through the center of the hexagons in the $[2\bar{1}\bar{1}]$ direction. Only where there are boundaries indicated by black arrows is the network disrupted in the $[2\bar{1}\bar{1}]$ direction. If one were to draw a line in the $[1\bar{2}1]$ direction, then, only the gray arrowed boundaries would be disruptive. The difference in symmetry of the molecular arrangements of the black and gray arrowed boundaries are shown in Fig. 2(b). Whether a boundary is of the black or gray, arrowed type does not affect the periodicity of

the network in the $[1\bar{1}0]$ direction and we therefore conclude that either boundary is equally probable and that they occur in a random sequence.

We conclude from our investigation that the Au(111)-$(22\times\sqrt{3})$ reconstruction causes a modification of the usual honeycomb PTCDI-melamine network so that an epitaxial relationship can be established. Regular boundaries of parallelogram shaped pores are introduced into the network which cause lattice matching in the $[1\bar{1}0]$ direction. The STM images do not show any isolated site on the surface that are particularly favorable for adsorption of PTCDI or melamine. This indicates that the total interaction between the network and the substrate is maximized by an epitaxial arrangement with all molecules contributing to a greater or lesser extent. If one were to think of melamine-PTCDI hexagons as distinct units, then the current scheme allows epitaxial ordering of these units. This ordering is long range and involves many competing molecule-molecule and molecule-substrate interactions. As the Au(111)-$(22\times\sqrt{3})$ reconstruction evolves from a misfit between the top two monolayers of the surface, it would be correct to state that the melamine-PTCDI network is epitaxial with a subsurface interface. This indicates a complexity of interaction that is unusual in epitaxial molecular systems.

We have also made an observation that is unrelated to network epitaxy. In the high resolution STM image in Fig. 2(b), patterns can be seen on the gold surface inside the empty hexagonal pores. The amplitude of these features is less than 0.2 Å high. This small corrugation indicates that this pattern may have an electronic origin. Low-dimensional structures on noble metals can act as electron-confining structures, and the amplitude distributions of the confined states can be observed using STM (Refs. 14–16) even at room temperature.[17] It is possible that the patterns in Fig. 2(b) corresponds to electron confinement inside the supramolecular pore network.

In this paper, we describe the formation of a PTCDI-melamine supramolecular network on a reconstructed Au(111)-$(22\times\sqrt{3})$ surface, and show that the reconstruction orders the network. Domain boundaries are observed on the Au fcc regions, creating a regular pattern of double hexagon rows separated by parallelogram pores. These results suggest that control of the Au(111) surface reconstruction using vicinal surfaces[1,18] could act as a new type of template for PTCDI and melamine supramolecular networks.

The authors thank the EPSRC (EP/D048761/1 and GR/S15808/01) for funding and C. Spencer (JEOL UK) for valuable technical support. We are grateful to P. Beton and L. Perdigao for helpful discussions.

[1] W. Xiao, P. Ruffieux, K. Ait-Mansour, O. Groning, K. Palotas, W. A. Hofer, P. Groning, and R. Fasel, J. Phys. Chem. B **110**, 21394 (2006).
[2] D. S. Deak, F. Silly, K. Porfyrakis, and M. R. Castell, J. Am. Chem. Soc. **128**, 13976 (2006).
[3] W. C. Wang, D. Y. Zhong, J. Zhu, F. Kalischewski, R. F. Dou, K. Wedeking, Y. Wang, A. Heuer, H. Fuchs, G. Erker, and L. F. Chi, Phys. Rev. Lett. **98**, 225504 (2007).
[4] D. S. Deak, F. Silly, K. Porfyrakis, and M. R. Castell, Nanotechnology **18**, 075301 (2007).
[5] J. V. Barth, Annu. Rev. Phys. Chem. **58**, 375 (2007).
[6] G. Schull, L. Douillard, C. Fiorini-Debuisschert, F. Charra, F. Mathevet, D. Kreher, and A.-J. Attias, Adv. Mater. (Weinheim, Ger.) **18**, 2954 (2006).
[7] J. A. Theobald, N. S. Oxtoby, M. A. Phillips, N. R. Champness, and P. H. Beton, Nature (London) **424**, 1029 (2003).
[8] L. Piot, A. Marchenko, J. Wu, K. Mullen, and D. Fichou, J. Am. Chem. Soc. **127**, 16245 (2006).
[9] D. Bonifazi, H. Spillmann, A. Kiebele, M. de Wild, P. Seiler, F. Cheng, H.-J. Guntherodt, T. Jung, and F. Diederich, Angew. Chem. **116**, 4863 (2004).
[10] F. Silly, A. Q. Shaw, P. Porfyrakis, G. A. D. Briggs, and M. R. Castell, Appl. Phys. Lett. **91**, 253109 (2007).
[11] L. M. A. Perdigao, E. W. Perkins, J. Ma, P. A. Staniec, B. L. Rogers, N. R. Champness, and P. H. Beton, J. Phys. Chem. B **110**, 12539 (2006).
[12] P. A. Staniec, L. M. A. Perdigao, A. Saywell, N. R. Champress, and P. H. Beton, ChemPhysChem **8**, 2177 (2007).
[13] J. V. Barth, H. Brune, G. Ertl, and R. Behm, Phys. Rev. B **42**, 9307 (1990).
[14] H. C. Manoharan, C. P. Lutz, and D. M. Eigler, Nature (London) **403**, 512 (2000).
[15] L. Niebergall, G. Rodary, H. F. Ding, D. Sander, V. S. Stepanyuk, P. Bruno, and J. Kirschner, Phys. Rev. B **74**, 195436 (2006).
[16] F. Silly, M. Pivetta, M. Ternes, F. Patthey, J. P. Pelz, and W.-D. Schneider, Phys. Rev. Lett. **92**, 016101 (2004); New J. Phys. **6**, 16 (2004).
[17] Ph. Avouris and I.-W. Lyo, Science **264**, 942 (1994).
[18] N. Weiss, T. Cren, M. Epple, S. Rusponi, G. Baudot, S. Rohart, A. Tejeda, V. Repain, S. Rousset, P. Ohresser, F. Scheurer, P. Bencok, and H. Brune, Phys. Rev. Lett. **95**, 157204 (2005).